



Integrative taxonomy reveals the presence of a new species of *Cyanea* (Scyphozoa: Discomedusae: Semaestomeae: Cyaneidae) from the West coast of Africa

YUSRA SAMSODIEN^{1,2}, MICHAEL K BROWN^{1,3} & MARK J GIBBONS^{1,*}

¹Department of Biodiversity and Conservation Biology, University of the Western Cape, Private Bag X17, Bellville 7535, South Africa.

²✉ yusrasamsodien25@gmail.com; <https://orcid.org/0000-0002-8087-9435>

³✉ mikeybrown@gmail.com; <https://orcid.org/0000-0002-3442-9601>

*Corresponding author: ✉ mgibbons@uwc.ac.za; <https://orcid.org/0000-0002-8320-8151>

Abstract

A new species of *Cyanea* is described from trawl samples collected in the Gulf of Guinea during 2017 and 2019. The species is a member of the *nozakii*-group, possessing interrupted radial septa, and is characterised by, *inter alia*, deeper rhopalial than velar marginal clefts, a uniformly papillose exumbrella, up to 200 tentacles per tentacle cluster and a dense network of anastomosing canals in broadly quadratic lappets. The species can be distinguished genetically from its congeners at both ITS1 and COI (minimum of 14.4% intergroup variation) regions as confirmed by multiple phylogenies and K2P analyses. This is the first record of a *nozakii*-group member in the Atlantic Ocean and the first description of the genus *Cyanea* from the west coast of Africa and the tropical Atlantic Ocean.

Key words: EAF Nansen Programme, lion's mane jellyfish

Introduction

At present, the genus *Cyanea* Péron & Lesueur, 1810 comprises 17 species of jellyfish and has the second greatest number of valid and recognised species in Semaestomeae Agassiz, 1862, after *Aurelia* Lamarck, 1816 (Collins & Morandini 2024). Both genera are uncommonly reported from the South and East Atlantic (Jarms & Morandini 2019; Gibbons *et al.* 2022 but see Lawley *et al.* 2021), though they are widely distributed in coastal waters across the Northern Hemisphere and in the Indo-Pacific. Both genera have been the subject of significant taxonomic confusion in the past, with respective type species, *Cyanea capillata* (Linnaeus, 1758) and *Aurelia aurita* (Linnaeus, 1758), being considered globally distributed (e.g. Kramp 1961) until relatively recently (e.g. Dawson 2005a).

According to Mayer (1910), Kramp (1960) and Jarms and Morandini (2019), species of *Cyanea* are characterised by adradial tentacles arranged in eight U-, or crescent-shaped groups that arise some distance from the bell margin on the subumbrella surface. On the subumbrella surface too are pronounced coronal muscles, arranged as a series of 16 “blocks” or fields that are separated by radial septa; the rhopalial fields being smaller than the tentacular ones. Sixteen fields of strong radial muscles extend from the coronal muscles to the base of the marginal lappets. The central mouth is broad and four-cornered and supports four, thin, curtain-like oral arms and the stomach extends peripherally as 16 gastric pouches that branch extensively into the lappets: four complexly folded inter-radial gonads hang pendulously from the subumbrella. The bell margin is generally divided into 16 broad lappets and supports eight, deep-set rhopalialia.

Species delimitation in the genus is difficult if it is based on morphological grounds alone. Historically, the species-specific diagnostic characters used included *inter alia* the number and arrangement of tentacles; the nature of the radial septa; the branching pattern of the canals in the marginal lappets and whether they intrude into the muscles or not; as well as the presence and distribution of nematocyst clusters on the exumbrella surface (Jarms & Morandini 2019). And colour, of course. Mayer (1910: 597) noted that “it is practically impossible to draw any fixed

distinctions between the various forms of the great *Cyanea* of the North Atlantic. Intergrading forms are commonly met with and many of the races are separated only geographically or upon colour distinctions which are neither wholly characteristic nor stable". Although later studies have shown reliable morphological features to distinguish different North Atlantic species (e.g. Russell 1970), similar observations (of confusion) at the global level were made more than one hundred years later by Jarms and Morandini (2019: 268): "It is impossible to reliably assess the number of valid species in the genus *Cyanea*. . . many representatives have been recorded with varying characters and uncertain distribution limits". That all said, Stiasny and van der Maaden (1943) have proposed that species within the genus *Cyanea* can be broadly separated into a *capillata*-group and a *nozakii*-group, on the basis that the latter has anastomosing connections between the tentacular and rhopaliar gastrovascular pouches, whilst the former does not.

Of the 17 species of *Cyanea* recognised as valid by Collins and Morandini (2024), the majority (11) were described prior to 1900. Fully 45% of these were inferred by Jarms and Morandini (2019) to be potentially *incertae sedis*, based on the poor and inconclusive nature of the original descriptions. The taxonomic confusion caused by "old" literature is not new, as clearly recognised by Mayer (1910) and more recently by (e.g.) Brown *et al.* (2021). While there may be a temptation to throw out morphology as a useful taxonomic tool in the face of poor material and replace it with molecular methods (e.g. Lawley *et al.* 2021), an integrative approach is preferred (Dawson 2005b; Brown & Gibbons 2022): the latter combining different threads of evidence to reach a consensus decision (morphology, meristics, molecules, ecology, etc.). Amongst the first of such studies to be published on Scyphozoa was that of Dawson (2005a), who focused on establishing the identity of *Cyanea* species off the east coast of Australia.

The only species of *Cyanea* formally described from West African coastal waters is *Cyanea annasethe* (Haeckel 1880), which was originally described as *Desmonema annasethe* Haeckel, 1880 from material collected west of South Africa by Wilhelm Bleek in 1877. This "...crumpled, brown..." specimen (Richards 2008) was illustrated in four near-monochrome figures on Plate XXX of Haeckel's *System der Acraspeden* in 1880 (Haeckel 1880). Figures 1 and 2 of this original plate were subsequently reworked, coloured and printed on Plate 8 of his *Kunstsformen der Natur* in 1899 (Haeckel 1899). The colours of the iconic images on Haeckel's (1899) Plate 8 (reproduced here as Figure 1), arguably the most famous jellyfish illustrations in the world, are not based on actual observations but were likely selected for aesthetic and artistic reasons; in keeping with the rest of the volumes he published in this series. That said, the images do impart some useful information regarding, *inter alia*, the distribution of papillae on the exumbrella, the relative depths of velar and rhopaliar marginal clefts, the numbers of tentacles, the arrangement of lappet canals, the base of the oral arms and the nature of the radial septa. It should be noted that the species was described from a single specimen off the SW coast of South Africa, and it has never been recaptured despite the area's inclusion in numerous regional scientific and fisheries surveys. Mayer (1910) considered *C. annasethe* a junior synonym of *Cyanea annaskala* von Lendenfeld, 1882, and neither Stiasny and van der Maaden (1943) nor Kramp (1961) recognised it as a valid species. But Gibbons *et al.* (2022: 80) have suggested the name be retained and that "further validation depends on the finding of more specimens and comparison with congeners".

More recently, several specimens of *Cyanea* have been collected off the West coast of Africa by the RV *Dr. Fridtjof Nansen* from pelagic and demersal trawls. Jellyfish have been given greater attention in the EAF Nansen Programme's activities around Africa since 2016 (FAO 2020), in part to encourage the establishment of regional baselines and in part to determine the presence of potentially new resources (Gibbons submitted). The specimens collected in these surveys are described in the present contribution, using the integrative approach combining morphological and molecular genetic methods.

Materials and methods

Sample collection and material examined

Thirty-eight *Cyanea* medusae were collected between Cote d'Ivoire and Angola in 2017 and 2019 by the RV *Dr. Fridtjof Nansen* using demersal or pelagic trawl nets (Figure 2). Two types of pelagic trawl nets were deployed, a smaller Åkratrawl with a mouth diameter of between 8 and 12 m and a larger Mulpelt 624 with a mouth opening of between 25 and 35 m: both nets had their cod-ends lined with a mesh of 4 mm. The demersal sampling gear comprised a Super Gisund bottom trawl, with a vertical opening of about 5.5 m and a distance between the wing tips

of 18 m during towing: the cod-end was lined with 10 mm mesh. On one occasion, a piece of oral arm tissue was immediately removed from a specimen for DNA analysis and placed in excess 96% ethanol (replaced three times in first 24 h) and stored in a freezer at -20°C. The balance of the material was preserved in 7 % seawater formalin for morphological analysis.

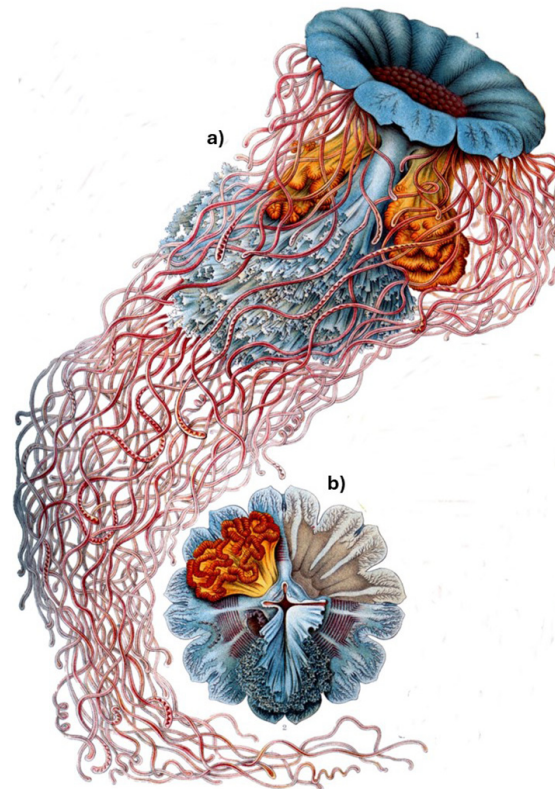


FIGURE 1. The only described species of *Cyanea* from the South Atlantic Ocean—*Cyanea annasethe* from off the west coast of South Africa. a) whole specimen in anteriolateral view, b) detail of subumbrella surface. Although the colours on Haeckel’s (1899) iconic image are not based on observations of a living specimen, the images do impart useful information regarding, *inter alia*, the distribution of papillae on the exumbrella, the relative depths of velar and rhopalial marginal clefts, the numbers of tentacles, the arrangement of lappet canals, the base of the oral arms and the nature of the radial septa. Note too the endodermal core to the tentacles. Adapted from Plate 8, Haeckel (1899).

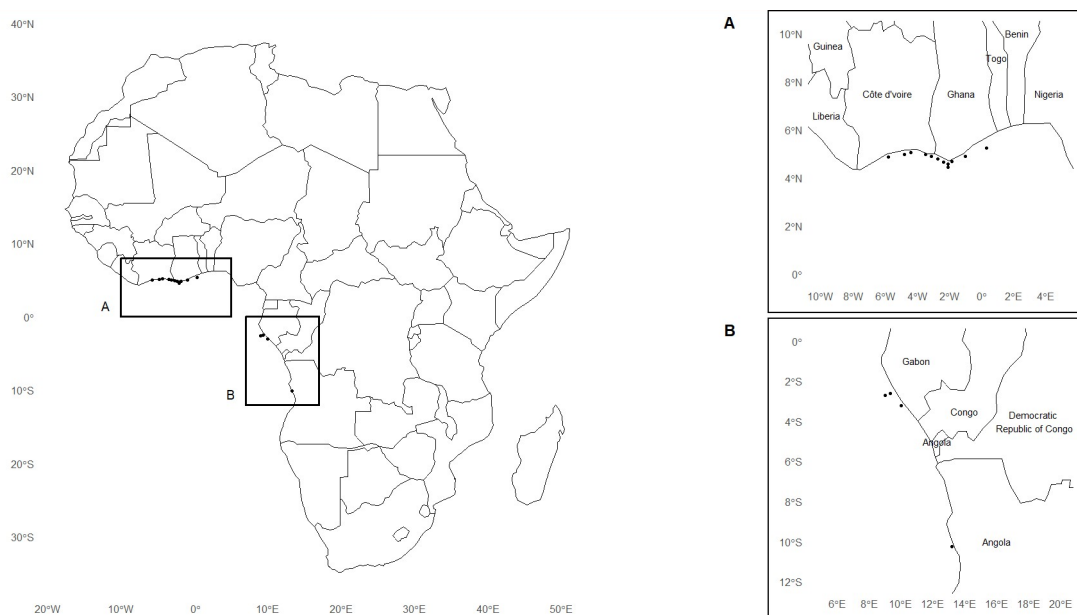


FIGURE 2. Map showing the location of samples collected, with details of the northern Gulf of Guinea (A) and West Africa (B).

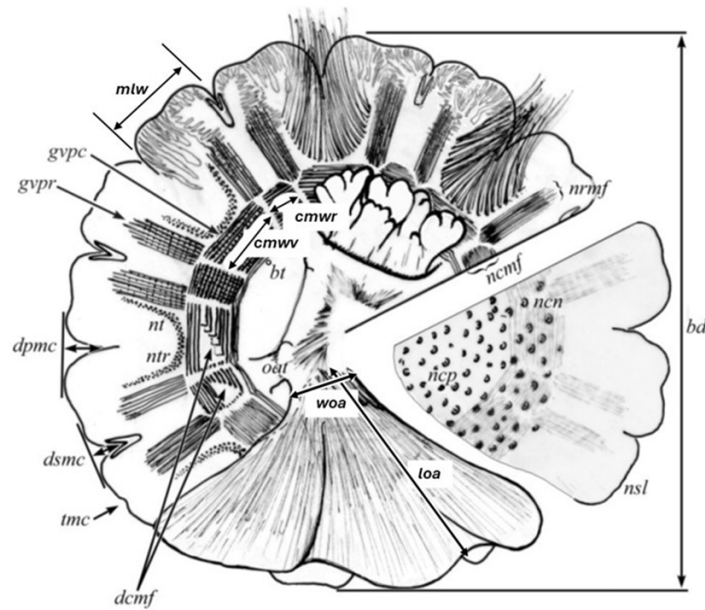


FIGURE 3. Diagram depicting the features that were counted or measured (mm) on *Cyanea* specimens collected from NW Africa (*bd* = bell diameter; *cmwr* = rhopalial coronal muscle width; *cmvw* = velar coronal muscle width; *dcmf* = depth of coronal muscle folds; *dpmc* = depth of primary marginal cleft; *dsmc* = depth of secondary marginal cleft; *gvpc* = gastrovascular pits in the coronal muscle folds; *gvpr* = gastrovascular pits in the radial muscle folds; *loa* = length of oral arms; *mlw* = marginal lappet width; *ncmf* = number of coronal muscle folds; *ncn* = number of nematocyst clusters; *ncp* = nematocyst clusters protrude; *nsl* = number of secondary lobes; *nt* = number of tentacles; *ntr* = number of tentacle rows; *tmc* = tertiary marginal cleft; *woa* = width of oral arms); adapted from Dawson (2005a).

Morphological, morphometric, and meristic data

No live specimens were described and all medusae were preserved. All material was examined a minimum of 3 years after initial collection (de Lafontaine and Legget 1989) and was soaked in freshwater for 24 h prior to inspection. Specimens were immersed in freshwater for examination, which took place on a light table, and measures were performed using Vernier callipers (Table 1 and Figure 3) with the assistance of a magnifying glass, where appropriate. Rhopalia were examined under a Leica S9i stereomicroscope. The morphological characters and morphometric counts are made based on Dawson (2005a) and are shown in Figure 3 and Table 1

The bell diameter (*bd*) of each specimen was determined using a tape-measure (mm), and the maximum bell thickness (*bt*) was assessed using Vernier calipers. The number of individual coronal (*ncmf*) and radial (*nrmf*) muscle folds was counted for each muscle field, and the average number per field then calculated for each muscle type per specimen: all fields were examined. The probing section of the Vernier callipers was placed between the pleats of the coronal muscle folds to determine the depth of the coronal muscle folds (*dcmf*), and the average depth was calculated per specimen. The depth of the primary (*dpmc*) and secondary (*dsmc*) marginal clefts was measured, and an average value of each measure was calculated for each specimen: all clefts were measured. The number of tentacle rows (*ntr*) in each of the 16 crescents was counted and averaged per specimen. The number of nematocyst clusters on the exumbrella (*ncn*) was not counted. The width of the marginal lappets (*mlw*) was measured, and an average value for each specimen was calculated. The width of velar (*cmvw*) and rhopalial (*cmwr*) muscle fields were measured, with average values calculated for each.

In addition to these continuous or ‘quantitative’ measurements, categorical or ‘discrete’ features were also examined. These included the presence/absence of gastrovascular pits in the coronal (*gvpc*) and radial (*gvpr*) muscle folds; the presence/absence of tertiary marginal clefts (*tmc*), the thickening of the oral arms at the basal area, and the presence and distribution of exumbrellar papillae. The length of the oral arms was measured, and the gastrovascular canals in the marginal lappets were viewed under a dissecting stereo microscope. Voucher specimens were deposited in the collection of the Iziko South African Museum (SAMC).

TABLE 1. The morphological and meristic characteristics measured (mm) or counted on specimens of *Cyanea* collected off the NW coast of Africa. See also Figure 2.

Abbreviation	Morphological characteristic description	Abbreviation	Morphological characteristic description
<i>bd</i>	Bell diameter	<i>mlw</i>	Marginal lappet width
<i>bt</i>	Maximum bell thickness	<i>ncmf</i>	Number of coronal muscle folds per field
<i>cmwr</i>	Rhopalial coronal muscle width	<i>ncn</i>	Number of nematocyst clusters
<i>cmwv</i>	Velar coronal muscle width	<i>nrmf</i>	Number of radial muscle folds per field
<i>dcmf</i>	Depth of coronal muscle folds	<i>nt</i>	Total number of tentacles per cluster
<i>dpmc</i>	Depth of primary marginal clefts	<i>ntr</i>	Number of tentacle rows per cluster
<i>dsmc</i>	Depth of secondary marginal clefts	<i>oat</i>	Oral arm thickness at base
<i>gvcf</i>	Gastrovascular intrusions in coronal muscle folds (+/-)	<i>tmc</i>	Tertiary clefts (+/-)
<i>gvrf</i>	Gastrovascular intrusions in radial muscle folds (+/-)	<i>woa</i>	Width of oral arm
<i>loa</i>	Length of oral arm		

Data analysis

Correlations between bell diameter and individual morphometric measures were computed to determine the effect of body size on measure size. Morphometric measures were then standardised against bell diameter. Those measures that proved to be size-independent, could then be used in multivariate comparisons with other species for which comparative data were available.

Unfortunately, such data are only available for *Cyanea rosea* Quoy & Gaimard, 1824 and *Cyanea annaskala*, and information for these were kindly provided by Prof M. Dawson (University of California, Merced, USA). Raw standardised values of isometric measures of specimens of *C. rosea*, *C. annaskala* and the material collected off West Africa were imported into PRIMER7 & PERMANOVA+ (Anderson *et al.* 2008), and a similarity matrix (Euclidean distance) was generated once they had been $\log(x + 1)$ transformed. To determine if there were differences in the multivariate characteristic of each species, both a Permutational MANOVA (PERMANOVA) (Anderson *et al.* 2008) and a Canonical Analysis of Principal Coordinates (CAP) (Anderson *et al.* 2008) were performed. PERMANOVAs and subsequent pairwise analyses allow for the comparison of characters from multiple a priori species and have the benefit of not necessarily requiring normal data. CAP analyses test the null hypothesis of no significant difference between species in multivariate space.

DNA analysis

DNA extraction, amplification, and sequencing

DNA was extracted following a modified CTAB protocol (Ras *et al.* 2020). Two gene regions, namely mitochondrial cytochrome *c* oxidase subunit I (COI), and nuclear internal transcribed spacer 1 (ITS1) were amplified from a single specimen using the primers listed in Table 2, using Polymerase Chain Reactions (PCR). A ramp-up cycle with the following reaction conditions was used when amplifying the COI gene region: 95°C for 4 min, 95°C for 2 min,

48°C for 1 min, 72°C for 2 min, followed by 10 cycles of 95°C for 2 min, 93°C for 45 sec, 50°C for 45 sec, 72°C for 1 min and 25 sec, followed by 35 cycles of 93°C for 45 sec, followed by a final step of 72°C for 10 min before holding at 4°C. A ramp-up cycle with the following reaction conditions was used when amplifying the ITS1 gene region: 95°C for 3 min, 95°C for 15 sec, 55°C for 15 sec, 72°C for 30 sec, followed by 35 cycles of 95°C for 15 sec, followed by a final step of 72°C for 7 min before holding at 4°C. Using 25 µl reaction volumes for all reactions, the PCR was performed on a BioRAD T100 thermal cycler. Following the PCR, two microliters of the resultant solution were examined on a 7% agarose gel. At the Central Analytical Facility located at the University of Stellenbosch, the cleaned products were cycle sequenced using BigDye chemistry and subsequently analysed with an ABI 3730 XL DNA Analyzer (Applied 514 Biosystems Inc.).

TABLE 2. The PCR primers used for the amplification of the cytochrome *c* oxidase subunit I (COI) and the nuclear Internal transcribed spacer 1 (ITS1) gene fragments used in the current study.

Gene Region	Primer Name	Sequence (5' – 3')	Reference
ITS1	jfITS1-5f	GGTTTCCGTAGGTGAACCTGCGGAAGGATC	Dawson and Jacobs 2001
	jfITS1-3r	CGCACGAGCCGAGTGATCCACCTTAGAAG	Dawson and Jacobs 2001
COI	LCOjf	GGTCAACAAATCATAAAGATATTGGAAC	Dawson 2005a
	HCO2198	TAAACTTCAGGGTGACCAAAAAATCA	Folmer <i>et al.</i> 1994

Sequence processing

BLASTn was used to compare DNA sequences with the GenBank nucleotide database to ensure that the correct sequences were utilised. DNA sequences for *C. annaskala*, *C. rosea*, *C. lamarckii* Péron & Lesueur, 1810, *C. capillata*, *Cyanea nozakii* Kishinouye, 1891, and *Cyanea tzetlinii* Kolbasova & Neretina, 2015 were downloaded as FASTA files from GenBank (Appendix 1). All sequences were processed in MEGA X (Tamura *et al.* 2021). Ambiguous bases were corrected based on the IUPAC nucleotide codes, and poorly defined terminal parts were eliminated. All sequences were then aligned using the alignment tool MUSCLE v.5.

Phylogenetic analyses

In the program PAUP v.4.0a169, the Akaike information criterion was applied to identify the “best fit model of evolution” for the COI (GTR + I + G), and ITS1 (GTR + I + G) gene regions. Bayesian analyses were then carried out in MrBayes v3.2.7 (Ronquist & Huelsenbeck 2003) and included one Monte Carlo Markov chain. The chains were sampled every 100th generation and a total of 200,000 generations were used. To summarise the resulting parameter values, the “sump” command was utilised. To determine whether there was adequate sampling of the data, the potential scale reduction factor (PSRF) was computed. In Mr. Bayes, the “sumt” command was then executed to summarise the trees. Trees were then visualised and adjusted in FigTree v.1.4.4 (<http://tree.bio.edu.ac.uk/software/gtree>).

Mean pairwise distances between species were calculated using the Kimura 2-parameter method. Using the “best fit model of evolution”, a maximum likelihood analysis was then carried out for both COI and ITS fragments. The bootstrap consensus tree was generated from 1000 permutations (Felsenstein 1985). Branches with less than 50% support were collapsed (Ras *et al.* 2020). The Neighbour-Join and BioNJ algorithms were automatically applied to a matrix of pairwise distances that were calculated using the Maximum Composite Likelihood (MCL) approach. Using these algorithms and the topology with the best log likelihood value, the initial tree(s) for the heuristic search was created. All evolutionary analyses were carried out in MEGA X.

Results

SYSTEMATICS

SUB-CLASS Discomedusae Haeckel, 1880

ORDER Semaestomeae L. Agassiz, 1862

FAMILY Cyaneidae L. Agassiz, 1862

GENUS *Cyanea* Péron and Lesueur, 1810

Cyanea altafissura sp. nov.

[TABLE 3; FIGURES 4–10]

Material examined. Holotype: Ghana: Gulf of Guinea (29.5 cm in diameter, 15 August 2019, in 7% formaldehyde in ambient seawater, area (4°N, 2°W), SAMC-A096867). **Paratypes:** Ghana: Gulf of Guinea (23.3 cm in diameter, 12 August 2019, preserved in 7% formaldehyde in ambient seawater, area (5°N, 0°W), SAMC-A096868); Côte d'Ivoire: Gulf of Guinea (22.2 cm in diameter, 4 August 2019, preserved in 7% formaldehyde in ambient seawater, area (4°N, 5°W), SAMC-A096869).

One specimen collected by the RV *Dr. Fridtjof Nansen* off Côte d'Ivoire on the 6th of August 2019 by bottom trawl at a sampling depth of 23 m (5.12°N, 4.75°W); Four specimens collected by the RV *Dr. Fridtjof Nansen* off Ghana on the on the 12th of August 2019 by bottom trawl at a depth of 28 m (5.05°N, 0.94°W); Three specimens collected by the RV *Dr. Fridtjof Nansen* off Accra off Ghana on the 13th of August 2019 by bottom trawl at a depth of 26 m (5.39°N, 0.36°W); Two specimens collected by the RV *Dr. Fridtjof Nansen* off Axim Ghana on the 9th of August 2019 by bottom trawl at a depth of 41 m (4.80°N, 2.30°W); Four specimens collected by the RV *Dr. Fridtjof Nansen* off Akwidaa, Ghana, on the 15th of August 2019 by bottom trawl at a depth of 26 m (4.72°N, 2.03°W); One specimens collected by the RV *Dr. Fridtjof Nansen* off Assouindé, Côte d'Ivoire on the 8th of August 2019 by bottom trawl at a depth of 25 m (5.13°N, 3.44°W); Four specimens collected by the RV *Dr. Fridtjof Nansen* off Takoradi, Ghana on the 10th of August 2019 by bottom trawl at a depth of 26 m (4.82°N, 1.78°W); One specimen collected by the RV *Dr. Fridtjof Nansen* off Akrou, Côte d'Ivoire on the 7th of August 2019 by bottom trawl at a depth of 25 m (5.19°N, 4.34°W); Four specimens collected by the RV *Dr. Fridtjof Nansen* off Gazéko, Côte d'Ivoire on the 5th of August 2019 by bottom trawl at a depth of 23 m (5°N, 5.73°W); Two specimens collected by the RV *Dr. Fridtjof Nansen* off New Town, Ghana on the 8th of August by a bottom trawl at a depth of 26 m (5.05°N, 3.08° W); One specimen collected by the RV *Dr. Fridtjof Nansen* off Akwidaa, Ghana on the 8th of August 2019 by bottom trawl at a depth of 25 m (4.59°N, 2.03° W); One specimen collected by the RV *Dr. Fridtjof Nansen* off Kanga, Ghana on the 28th of September 2019 by pelagic trawl at a depth of 33 m (4.94°N, 2.68° W); One specimen was collected by the RV *Dr. Fridtjof Nansen* off Nyanga, Gabon, on the 26th of September 2017 by bottom trawl at a depth of 41 m (3.06°S, 10.04°E); One specimen was collected by the RV *Dr. Fridtjof Nansen* off Gabon on the 25th of September 2017 by trawl at a depth of 46 m (2.48°S, 9.39°E); One specimen was collected by the RV *Dr. Fridtjof Nansen* off Gabon, on the 24th of September 2017 by bottom trawl at a depth of 118 m (2.57°S, 9.06°E); One specimen was collected by the RV *Dr. Fridtjof Nansen* off Nyanga, Gabon, on the 26th of September 2017 by bottom trawl at a depth of 41 m (3.06°S, 10.04°E); Four specimens were collected by the RV *Dr. Fridtjof Nansen* off the coast of Angola, on the 16th of October 2017 by pelagic trawl at a depth of 20 m (10.11°S, 13.34°E)

Type locality. Akwidaa, Ahanta West Municipal District, Ghana

Distribution. Range extends around the Gulf of Guinea, West Africa, from Côte d'Ivoire to Gabon and southwards to central Angola.

Diagnosis. Medium-sized *Cyanea*; exumbrella surface slightly papillose throughout; 16 rectangular marginal lobes; rhopalial clefts deeper than velar clefts; radial and coronal muscle fields prominent, without gastrovascular intrusions, with 5 and 7 muscle folds respectively. With up to 200 strap-like, hollow tentacles arranged in eight U-shaped fields or clusters. Rhopalium small; statocyst on short stalk lacking bulbs/warts located at base of long, tubular rhopalial pit. Mouth arms greatly thickened basally; gastrovascular sinus in 16 lobes separated by interrupted septa of the *nozakii* type, penetrating marginal lappets on a broad front as a fine network of branching and anastomosing canals.

Biological data: Found at depths between 20–118 m.

Etymology. *altafissura*, Latin, refers to the comparatively deep depth of the rhopalial cleft.

Holotype description. Umbrella a flattened hemisphere with a diameter of 295 mm; thickest centrally and thinning to margin. Exumbrella light brown in colour, with nematocyst warts that impart a rough surface texture throughout (papillose). Umbrella margin divided into 16, broad and approximately quadratic lappets, 44.8 mm in width; two lappets per octant; (secondary) clefts between rhopalial lappets deeper than those between (primary) velar lappets. Coronal muscle in 16 fields, rhopalial fields (9.8 mm) narrower than velar (18.4 mm) fields; each field separated from neighbour by prominent thickened septal ridge; fields with 7–11 coronal muscle folds. Radial muscles in 16 fields extending distally from coronal muscles to bell margin, not into lappets, each field with 3–6 muscle folds. Coronal and radial muscles without gastrovascular pits. With eight rhopalia, each situated at base of long pit, protected by margins of neighbouring lappets; statocyst at end of short, smooth rhopalial stalk, which lacks a basal bulb. Eight, deep adradial U-shaped tentacle bundles situated between radial muscle fields opposite velar lappets; tentacle bundles comprised of three rows of tentacles proximally but a single row distally; tentacle bundles span the entire length of the radial muscle fields; tentacles hollow, between 160–190 in number, largest proximally and smallest distally. Mouth broadly quadratic with four oral arms, thickened at base; thin, curtain-like tissue extending between oral arms; shorter than the bell diameter. Central stomach without septa or gastric cirri; extending to bell margin as 16 gastric pouches, separated by interrupted septa of the *nozakii* type, penetrating lappets on a broad front as dendritic canals, with obvious anastomoses. Gonads complexly folded, cream in colour, pendulous; attached to the subumbrella.

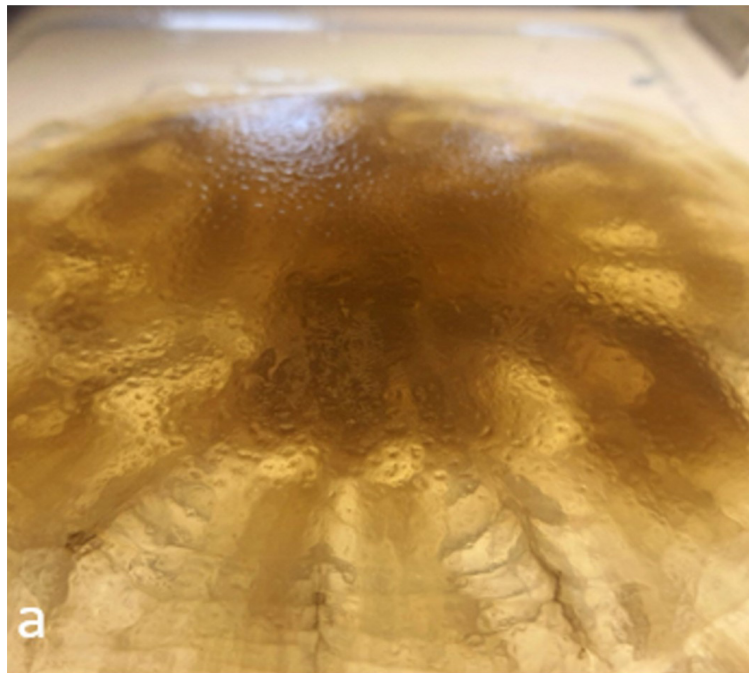


FIGURE 4. *Cyanea altafissura* sp. nov. a) Exumbrella surface showing uniform distribution of nematocyst warts.

Description of other specimens and additional data

Medusae: The bell colour was light brown or beige, although one specimen had purple oral arms and gonads. Bell a flattened saucer; thicker at the centre and thin at the periphery; maximum bell thickness increasing with increasing bell diameter (Table 3). Exumbrella surface texture slightly rough throughout (Figure 4). Bell margin divided into 16 broad, rectangular lappets of approximately similar size and shape (Figure 5); lappet width increases isometrically with bell diameter; each approximately 16% bell diameter in width; the depth of the (primary) velar and (secondary) rhopalial marginal clefts increases with increasing bell diameter (Table 3), isometric; standardised depth of rhopalial clefts (mean = 0.09, SE = 0.006, n = 22) significantly deeper than velar clefts (mean = 0.06, SE = 0.005; n = 22) ($F = 17.012$, $p = 0.0005$). Only four of the thirty-eight analysed individuals (~10%) had tertiary clefts, dividing the bell margin into 32 marginal lobes.

TABLE 3. Raw and standardised morphometric measures of *Cyanea altafissura* sp. nov. in the Gulf of Guinea. Bold values indicate significant ($p < 0.01$) correlations between measure and bell diameter. See Figure 2.

Abbreviation	Morphological characteristic description	Raw					Standardised				
		Mean	Standard deviation	n	Max	Min	Mean	Standard deviation	n	Max	Min
<i>bd</i>	Bell diameter (mm)	206,42	70,42	38	382	89					
<i>bt</i>	Maximum bell thickness (mm)	16,55	7,92	38	36,53	1,67	0,078	0,030	38	0,155	0,018
<i>cmwr</i>	Rhopalial coronal muscle width (mm)	9,49	3,40	7	13,88	4,88					
<i>cmvw</i>	Velar coronal muscle width (mm)	18,04	3,95	7	23,06	11,13					
<i>cmvw:cmwr</i>	Velar : Rhopalial coronal muscle width	2,00	0,38	7	2,68	1,66					
<i>dcmf</i>	Depth of coronal muscle folds (mm)	5,30	3,17	38	13,87	1	0,024	0,012	38	0,058	0,009
<i>dpmc</i>	Depth of primary marginal clefts (mm)	12,85	7,28	32	37,8	3,13	0,060	0,021	32	0,101	0,013
<i>dsmc</i>	Depth of secondary marginal clefts (mm)	19,08	9,29	32	43	2,44	0,089	0,024	32	0,137	0,010
<i>loa</i>	Length oral arms (mm)	85,83	44,70	28	220,00	35,50	0,375	0,200	28	0,861	0,160
<i>mlw</i>	Marginal lappet width (mm)	36,79	6,71	6	44,79	28,93	0,151	0,009	6	0,165	0,138
<i>ncmf</i>	Number of coronal muscle folds per field	7,38	1,04	38	9,69	5,4	0,041	0,017	38	0,079	0,019
<i>nrnf</i>	Number of radial muscle folds per field	4,38	0,73	38	6,13	3	0,024	0,008	38	0,043	0,013
<i>ntr</i>	Number of tentacle rows per cluster	2,14	0,42	37	3	1					
<i>woa</i>	Width oral arms (mm)	28,28	7,91	28	50,25	14,50	0,125	0,048	28	0,246	0,083

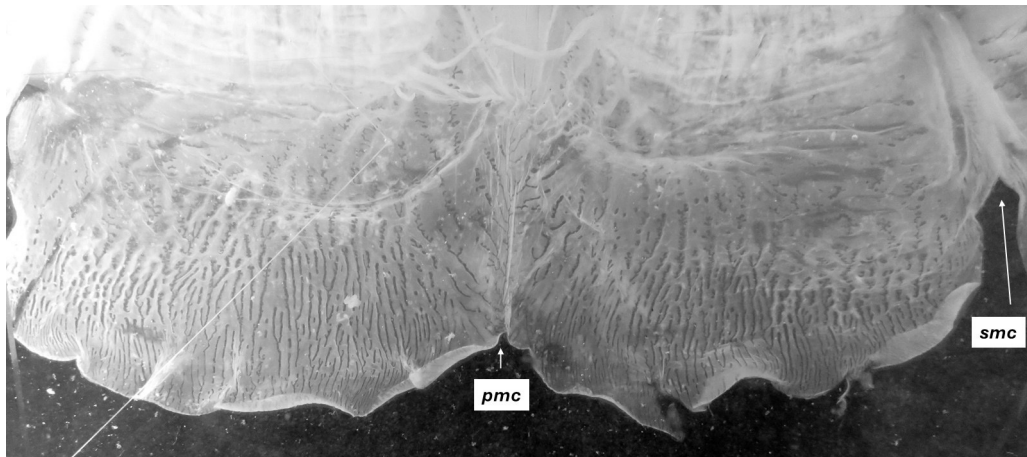


FIGURE 5. *Cyanea altafissura* sp. nov. View of subumbrella showing rectangular shape of marginal lappets, the comparative depths of the primary/velar (*pmc*) and secondary/rhopalial (*smc*) clefts, and the dendritic and anastomosing nature of marginal canals.

Rhopalium relatively small; statocyst on a short, smooth stalk lacking basal bulbs, papillae or other protuberances (Figure 6); located at the base of long tube-like pit, bounded on the exumbrella surface by a hood formed from the fusion of neighbouring lappet edges, and on the subumbrella surface by overlapping lappet margins (Figure 6); ocelli not observed.

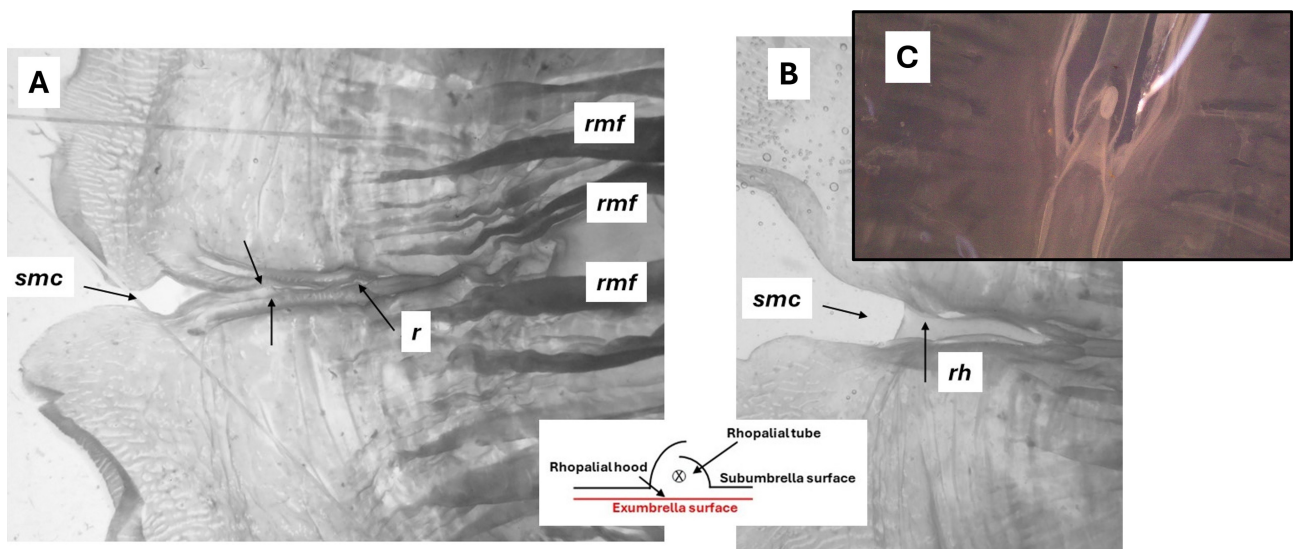


FIGURE 6. *Cyanea altafissura* sp. nov. A) Subumbrella view of the bell margin, showing a secondary marginal cleft (*smc*), the position of radial muscle fields (*rmf*), the rhopalium (*r*) and the overlapping edges of the marginal lappets that in effect form a rhopalial tube (see schematic inset). B) subumbrella view of bell margin showing a secondary marginal cleft (*smc*) and the rhopalial hood (*rh*). C) detail of rhopalium at base of rhopalial “tube”, note the absence of bulbs/papillae on stalk.

Sixteen coronal muscle fields, each field separated from neighbour by prominent thickened septal ridge (Figure 7); rhopalial fields (mean = 4% bell diameter, SE = 0.2%, n = 68) significantly narrower than velar (mean = 7.2% bell diameter, SE = 0.2%, n = 67) ($F = 182.86, p < 0.0005$). Number of muscle folds per field varying from between 4–14 (mode = 7) in a size independent way, as too does the depth of individual muscle folds (mean = 6.5 mm, SE = 0.1 mm). Radial muscles in 16 fields, extending from a position between rhopalial and velar coronal muscles towards base of lappets at bell margin (Figure 7); with between 3–8 muscle folds (mode = 5) proximally, fanning out to a greater number distally. Gastrovascular pits in the coronal and radial muscle folds absent.

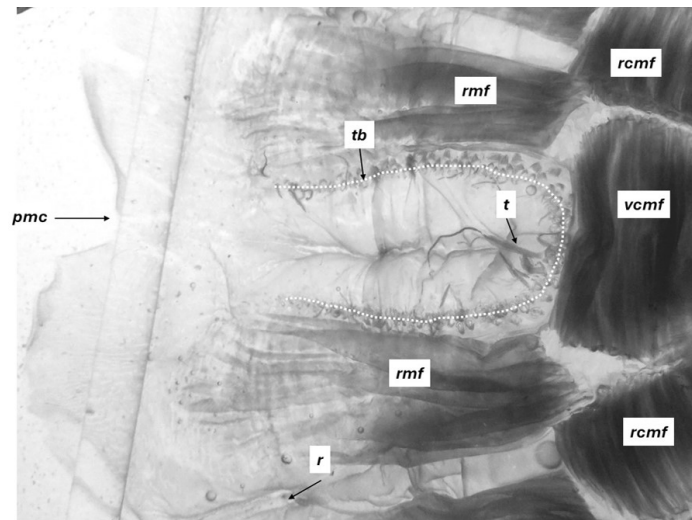


FIGURE 7. *Cyanea altafissura* sp. nov. Subumbrella view of U-shaped tentacular bundle (*tb*), hollow tentacle (*t*), velar (*vcmf*) and rhopalial (*rcmf*) coronal muscle fields, radial muscle fields (*rmf*), primary marginal cleft (*pmc*) and rhopalium (*r*).

Tentacles arranged in eight, deeply rectangular, U-shaped bundles that extend from distal edge of coronal muscles towards base of lappets (Figure 7); tentacle bases very close to each other, and distinct rows hard to observe clearly, especially proximally. As a rule, tentacles in a single row towards bell margin and clustered in up to four rows adjacent to coronal muscle fields. Tentacles hollow, strap-like (Figure 7) and with a clear endodermal core. Proximal tentacles longer and thicker than distal ones. Up to 200 tentacles per field, size dependant.

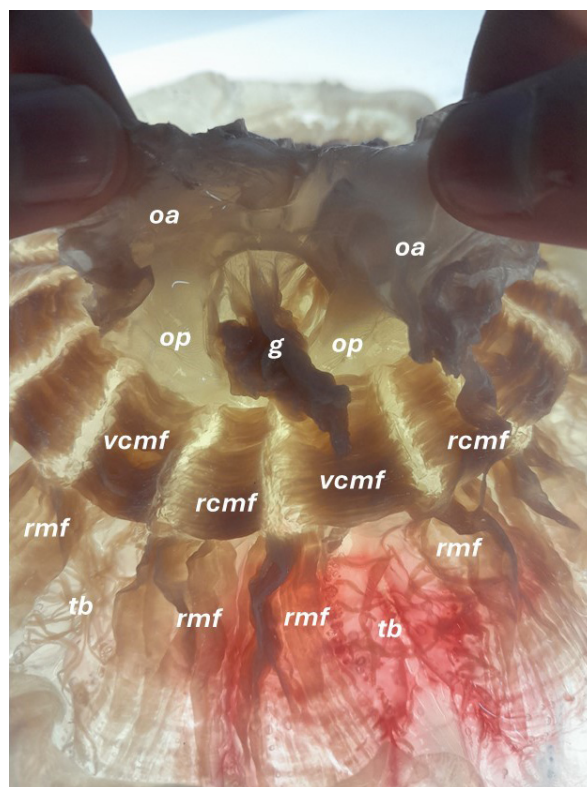


FIGURE 8. *Cyanea altafissura* sp. nov. Subumbrella view showing one of the four gonads (*g*) emerging from between adjacent oral pillars (*op*) at base of oral arms (*oa*). Velar (*vcmf*) and rhopalial (*rcmf*) coronal muscle fields, radial muscle fields (*rmf*) and tentacle bundles (*tb*) also shown.

The mesoglea at the base of the manubrium a strongly thickened ring (Table 3) supporting four oral arms on short pillars (Figure 8); oral arms greatly expanded laterally, membranous and curtain-like. Unfortunately, it was not possible to accurately measure oral arm length, but generally shorter than diameter of bell. Mouth approximately quadratic in shape; stomach without septa; small specimens with numerous short gastric cirri arranged in four inter-radial groups attached to subumbrella (Figure 9). Stomach extending to bell margin as 16 gastric pouches that penetrate lappets on a broad front as a network of fine dendritic canals, with obvious anastomoses (Figure 5); pouches separated by indistinct septa distal of coronal muscle fields that are interrupted and of the *nozakii*-type (Figure 10) with anastomosing connections between the tentacular and rhopalial gastrovascular pouches. Four, complex, folded gonads originate from stomach wall, and emerge from between the thickened bases of adjacent oral pillars (Figure 8) to hang freely below subumbrella, decumbent.

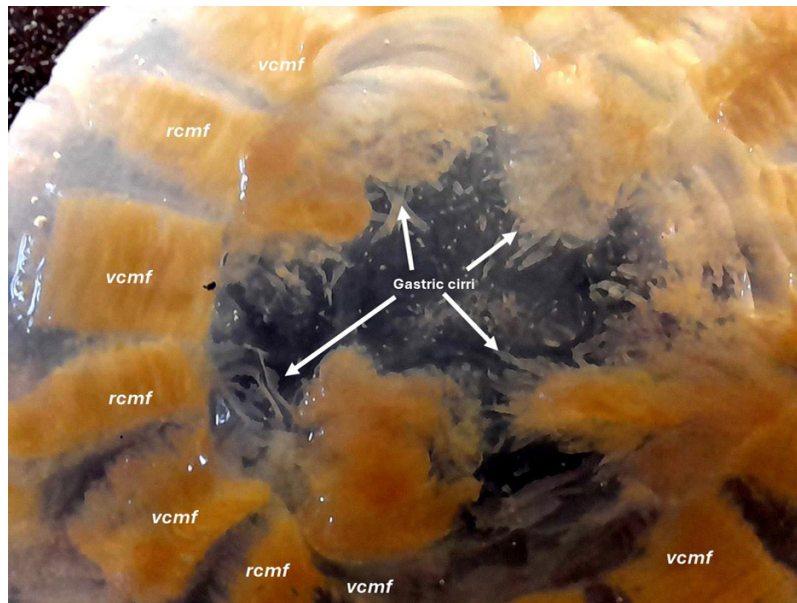


FIGURE 9. *Cyanea altafissura* sp. nov. Subumbrella view, showing coronal muscle fields and inter-radial gastric cirri.

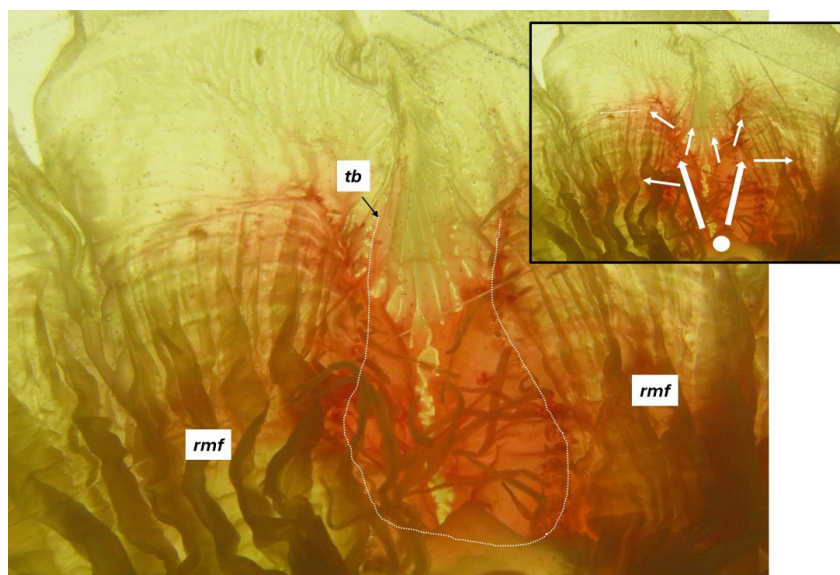


FIGURE 10. *Cyanea altafissura* sp. nov. Subumbrella view of gastric sinus running beneath radial muscle fields (*rmf*) and tentacular bundle (*tb*), highlighted by red dye. Inset shows point of dye injection (circle) and subsequent movement through anastomosing connections between the tentacular and rhopalial gastrovascular pouches.

Molecular analysis

The species is distinguished by both COI and ITS1 gene regions with 11.7% minimum COI intergroup distance to its nearest sister. Nuclear regions show an even clearer distinction with *C. altafissura* **sp. nov.** sitting basal to the rest of the *Cyanea* clade.

TABLE 4. Results of the PERMANOVA analysis and pairwise comparisons test comparing the standardised morphometric measurements of *Cyanea annaskala*, *Cyanea rosea* and *Cyanea altafissura* **sp. nov.**

PERMANOVA						
	Df	SS	MS	F	Unique perms	Pr (MC)
Species	2	0.04	0.02	13.95	999	0.001
Residual	39	0.06	0.001			
Total	41	0.1				
Pairwise comparisons test						
Species Groups		T		Unique perms		Pr (MC)
<i>Cyanea annaskala</i>	<i>Cyanea altafissura</i> sp. nov.	4.13		998		0.001
<i>Cyanea rosea</i>	<i>Cyanea altafissura</i> sp. nov.	3.44		992		0.001

Remarks and Discussion

The Maximum likelihood (ML) analysis of the COI data revealed three monophyletic lineages (Figure 11, Appendix 3), which supports the separation of all known *Cyanea* species and *C. altafissura* **sp. nov.** (minimum pairwise differences = 11.7%) (Table 5, Appendix 2). This divergence is in line with species distinctions of many other Scyphozoa (Scorrano *et al.* 2017; Ras *et al.* 2020; Brown *et al.* 2021). The ML analysis of COI places the West African species as a sister group to *C. nozakii*. In contrast, ML analyses of the ITS1 data revealed the presence of two monophyletic lineages (Figure 12), which placed *C. altafissura* **sp. nov.** in its own lineage, with *C. capillata*, *C. rosea*, *C. tzetlinii*, and *C. nozakii* forming one monophyletic clade (minimum pairwise differences = 14.4%).

TABLE 5. Mean pairwise genetic distances between the mtDNA (COI) and nuDNA (ITS1) sequences of *Cyanea altafissura* **sp. nov.** and other recognised species of *Cyanea* in GenBank. Distances are represented as mean \pm standard error. Pairwise genetic distances between all *Cyanea* species are provided in the supplementary tables.

Species comparisons		nuDNA	mtDNA
<i>Cyanea altafissura</i> sp. nov.	<i>Cyanea annaskala</i>	0.221 \pm 0.048	0.131 \pm 0.021
<i>Cyanea altafissura</i> sp. nov.	<i>Cyanea rosea</i>	0.221 \pm 0.048	0.127 \pm 0.019
<i>Cyanea altafissura</i> sp. nov.	<i>Cyanea tzetlinii</i>	0.149 \pm 0.021	0.136 \pm 0.021
<i>Cyanea altafissura</i> sp. nov.	<i>Cyanea nozakii</i>	0.144 \pm 0.029	0.133 \pm 0.019
<i>Cyanea altafissura</i> sp. nov.	<i>Cyanea capillata</i>	0.162 \pm 0.023	0.139 \pm 0.022
<i>Cyanea altafissura</i> sp. nov.	<i>Cyanea lamarckii</i>	-	0.129 \pm 0.02

The Bayesian analysis of the ITS1 data revealed two monophyletic lineages between *C. altafissura* **sp. nov.** and *C. capillata*, *C. rosea*, *C. tzetlinii*, and *C. nozakii*. Notably, the mitochondrial DNA sequence data showed less variation between the West African species and *C. nozakii*, with the two forming a monophyletic clade (Figure 11). In contrast, nuclear DNA sequence data showed greater variation (Table 5) between *C. altafissura* **sp. nov.** and *C. nozakii*, with *C. altafissura* **sp. nov.** sitting as its own monophyletic group, sister to all other *Cyanea* species. This is in part because the pairwise genetic distances between the West African *Cyanea* and other *Cyanea* species are higher for nuDNA (ITS1) than for mtDNA (COI).

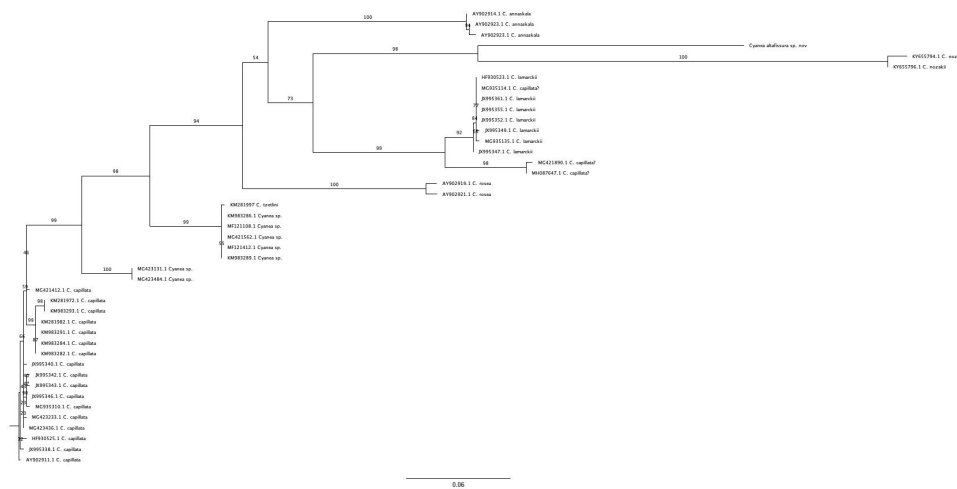


FIGURE 11. Rooted Maximum Likelihood COI tree using GTR + I + G model of evolution: North Atlantic Ocean, red; Tropical Atlantic Ocean, black; South Pacific Ocean, blue; Indian Ocean, orange. Bootstrap support values (ML) are given above branches, with posterior probabilities (BY) given below branches.

Greater genetic distances are often associated with the mitochondrial DNA (mtDNA), a result of its faster evolutionary rate when compared to nuclear DNA (nuDNA) (Hellberg 2006; Eytan 2009). While a relatively reduced evolutionary rate in the mtDNA of scyphozoans has not been observed, it has been reported for several anthozoan species (Hellberg 2006; Eytan 2009). Low levels of mtDNA variation can be the result of expanding geographical ranges, which lead to intensified founder effects (Hellberg 2006). During range expansions, a reduced population size of mtDNA genes may lead to a relatively lower genetic diversity in the new population. Intensified founder effects as a result of range expansions could therefore provide an alternative explanation for the slightly lower variation in the mtDNA between *Cyanea* species when compared to nuDNA. It is also not surprising that *C. altafissura* **sp. nov.** sits basal to other species within the *Cyanea* clade. It is a trend observed in Brown *et al.* (2021) and Ras *et al.* (unpublished data). While hypotheses for this have not yet been tested, it is quite likely due to a combination of factors including the presence of the upwelling systems along the west coast of Africa, the Agulhas Current on the east coast of Africa, the divergence time of the African continent and the massive freshwater outflows along the coast of Africa leading to relatively isolated ecosystems with little chance of geneflow (as mentioned in Brown *et al.* 2021).

Unfortunately, owing to the paucity of quantitative descriptions of *Cyanea* in the literature, it is not possible to statistically compare the morphometrics of *C. altafissura* **sp. nov.** with those of others in the genus, even using the null model approach proposed by Brown and Gibbons (2021): except for *C. rosea* and *C. annaskala*. The results of the PERMANOVA indicate that, with the few common measures used, there are significant morphometric differences between *C. altafissura* **sp. nov.**, *C. rosea*, and *C. annaskala* (Table 4). Indeed, *C. altafissura* **sp. nov.** is clearly separated from the other two species on the first CAP axis, with the second CAP axis separating *C. rosea* from *C. annaskala* (Figure 13). Correlation values associated with the eigenvalues are high for CAP 1, but relatively low for CAP 2 ($\delta_1^2 = 0.93$, $\delta_2^2 = 0.41$). While 95.24% of all *Cyanea* specimens were correctly assigned to the appropriate taxon, two samples were misclassified: one specimen of both *C. annaskala* and *C. altafissura* **sp. nov.** were incorrectly assigned to *C. rosea*.

Table 6 summarises the morphological features described for all *Cyanea* species, as well as *C. altafissura* **sp. nov.** It is immediately clear from this table that comparable observations have not been made for all species, which complicates firm conclusions about identity. Although an inspection of relevant type materials is ideally needed to confirm identity, we believe that it is not needed here because: a) no other species of *Cyanea* have previously been described from the tropical coast of West Africa; b) most species of this genus appear to have restricted distributions (Jarms & Morandini 2019); and c) *Cyanea altafissura* **sp. nov.** is morphologically distinct from other species that are geographically “closest” to the type locality (see below). While the genetic data collected indicate that *Cyanea altafissura* **sp. nov.** is distinct from all other identified species of *Cyanea* at present in GenBank, this point is moot given that most species have yet to be barcoded. This is a wake-up call for modern descriptions of all known species to be made.

TABLE 6. Morphological features that allow for the differentiation of currently recognised species of *Cyanea*. Modal numbers of measures reported for *C. altafissura sp. nov.*, where appropriate; --, no data.

Species	<i>C. annaskala</i>	<i>C. capillata</i>	<i>C. rosea</i>	<i>C. altafissura sp. nov.</i>	<i>C. lamareckii</i>	<i>C. nozakii</i>
Distribution	SE Australia	NE Atlantic	East Australia	Tropical W Atlantic	NE Atlantic	Indo-Pacific
Number circular muscle folds	17–24	13–15	11–14	4–14 (mode 7)	16–20	9–10
Number radial muscle folds	7–18	3–6	8–12	3–8 (mode 5)	5–10	5
Number tentacle rows	3–4	4	--	1–4	4	--
Number tentacles per octant	150	70–150	--	<200	20–70	100
Tertiary cleft	Yes	No	No	Occasionally	No	No
Rhopalial bulb	--	Absent	--	Absent	Absent	Absent
Rhopalial ocellus	--	Absent	--	Absent	Absent	Absent
Lappet shape	Bifurcate	Bifurcate	Bifurcate	Rectangular	Bifurcate	Rectangular
Lappet cleft	Velar > Rhopalial	Velar > Rhopalial	Velar > Rhopalial	Rhopalial > Velar	Velar > Rhopalial	Velar > Rhopalial
Anastomoses in peripheral canals	No	Rarely	--	Extensive	No	Yes
Pits in muscle folds	Absent	Present	Present	Absent	Absent	Absent
Exumbrella papillae	Mostly at centre	Only at margin	Mostly at centre	Evenly distributed	Mostly at centre	Mostly at centre
Septum type	--	<i>capillata</i>	<i>capillata</i>	<i>nozakii</i>	<i>capillata</i>	<i>nozakii</i>
Maximum bell diameter (cm)	35	<200	25	<38	<30	<120
Source	Mayer (1910) Gershwin <i>et al.</i> (2010) Dawson (2015)	Russell (1970) Dawson (2015) Gershwin <i>et al.</i> (2010) Kolbasova <i>et al.</i> (2015)	Quoy & Gaimard (1824) Dawson (2015) Gershwin <i>et al.</i> (2010) Kolbasova <i>et al.</i> (2015)	This paper	Russell (1970) Gershwin <i>et al.</i> (2010) Kolbasova <i>et al.</i> (2015)	Stiansy & van der Maaden (1943) Dong <i>et al.</i> (2008) Gershwin <i>et al.</i> (2010)

.....Continued on the next page

TABLE 6. (Continued)

Species	<i>C. tzetlinii</i>	<i>C. annasethe</i>	<i>C. mullerianthe</i>	<i>C. mjobergi</i>	<i>C. buitendijki</i>	<i>C. versicolor</i>
Distribution	White Sea	SE Atlantic	S Australia	W Australia	Malayan Archipelago	NW Atlantic
Number circular muscle folds	--	8	15–18	6–7	7–9	--
Number radial muscle folds	--	4–6	--	4–5	--	--
Number tentacle rows	--	1	--	3–6	5	--
Number tentacles per octant	20–65	13–17	150	--	150	--
Tertiary cleft	Yes	No	Yes	No	No	--
Rhopalial bulb	Present	--	--	--	--	--
Rhopalial ocellus	Present	--	--	--	--	--
Lappets	Rounded	Rounded	Bifurcate	Rounded	Rounded	Square
Lappet cleft	Velar > Rhopalial	Velar > Rhopalial	--	Velar > Rhopalial	Velar > Rhopalial	--
Anastomoses in peripheral canals	No	Dendritic	--	Dendritic: No	No	--
Pits in muscle folds	Present	Absent	Absent	Absent	Absent	--
Exumbrella papillae	Only at margin	--	Smooth	Smooth	Only at centre	Smooth
Septum type	<i>capillata</i>	<i>capillata</i>	<i>capillata</i>	<i>nozakii</i>	<i>nozakii</i>	<i>capillata</i>
Maximum bell diameter (cm)	17	10	10	14	31	10
Source	Kolbasova <i>et al.</i> (2015)	Haeckel (1880)	Haacke (1887) Gershwin <i>et al.</i> (2010)	Stiasny (1921) Stiasny & van der Maaden (1943) Gershwin <i>et al.</i> (2010)	Stiasny (1919) Stiasny & van der Maaden (1943) Gershwin <i>et al.</i> (2010)	Agassiz (1862)

..... Continued on the next page

TABLE 6. (Continued)

Species	<i>C. barkeri</i>	<i>C. purpurea</i>	<i>C. ferruginea</i>	<i>C. postelsi</i>	<i>C. citrea</i>	<i>C. fulva</i>
Distribution	E Australia	NW Pacific	N Pacific	N Pacific	NW Pacific	NW Atlantic
Number circular muscle folds	7–10	13	--	--	15	--
Number radial muscle folds	6–7	12	--	--	14	--
Number tentacle rows	6	5	--	--	3–4	--
Number tentacles per octant	300	--	--	--	--	--
Tertiary cleft	--	No	No	Yes	Yes	Yes
Rhopalial bulb	--	--	Absent	Absent	Absent	--
Rhopalial ocellus	--	--	--	--	--	--
Lappets	--	Square	Square	Rounded	Rounded	Rounded
Lappet cleft	--	Velar > Rhopalial	Velar > Rhopalial	--	Velar > Rhopalial	--
Anastomoses in peripheral canals	--	Yes	No	--	Rare	--
Pits in muscle folds	Absent	Present	Absent	--	Present	Absent
Exumbrella papillae	Smooth	--	--	--	--	Present
Septum type	nozakii	capillata	capillata	capillata	capillata	capillata
Maximum bell diameter (cm)	<40	36	45	<200	30	20
Source	Gershwin <i>et al.</i> (2010)	Kishinouye (1902) Kishinouye (1910)	Eschscholtz (1829) Stiasny (1943) Kolbasova <i>et al.</i> (2015)	Brandt (1835) Kolbasova <i>et al.</i> (2015)	Kishinouye (1902) Kishinouye (1910) Kolbasova <i>et al.</i> (2015)	Agassiz (1862) Calder (2009) Holst and Laakmann (2014)

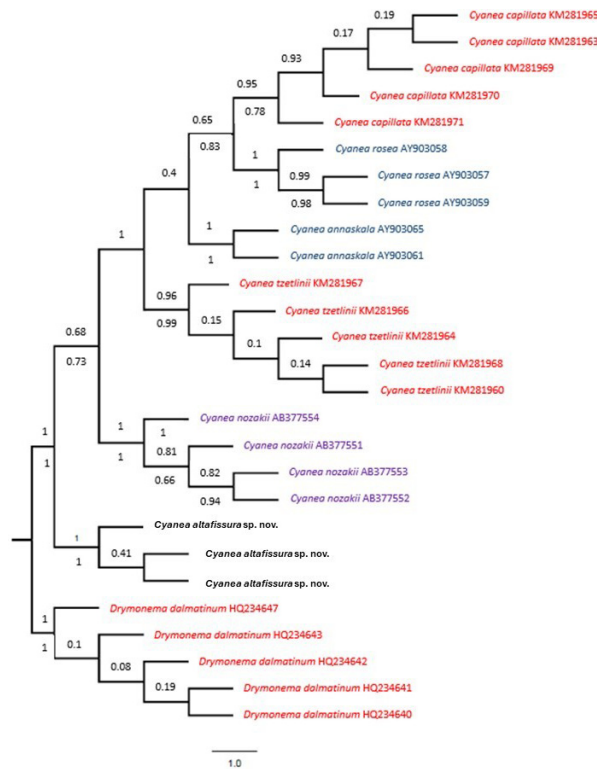


FIGURE 12: Rooted Maximum likelihood ITS1 tree using the GTR + I + G model of evolution: North Atlantic Ocean, red; Tropical Atlantic Ocean, black; South Pacific Ocean, blue; Pacific Ocean, purple. Bootstrap support values (ML) are given above branches, with posterior probabilities (BY) given below branches.

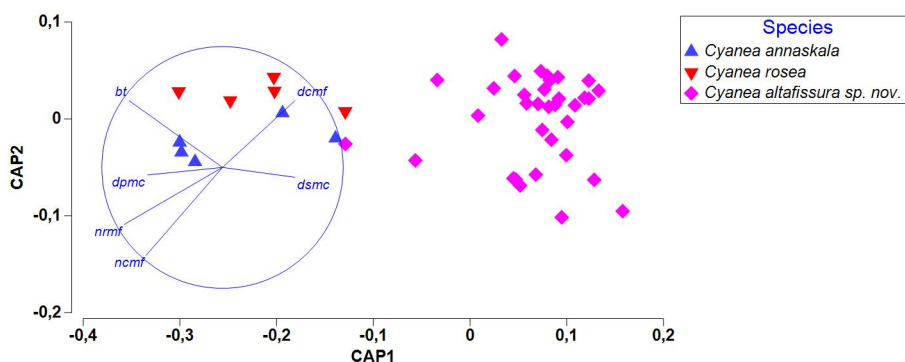


FIGURE 13. Canonical Analysis of Principal Coordinates for six standardised and isometric measures of *Cyanea annaskala*, *Cyanea rosea* and *Cyanea altafissura* sp. nov. Values for CAP1 and CAP2 were 0.93 and 0.41 respectively. (*bt* = bell thickness; *dcmf* = depth of coronal muscle folds; *dsmc* = depth of secondary marginal cleft, *dpmc* = depth of primary marginal cleft; *nrmf* = number of radial muscle folds; *ncmf* = number of coronal muscle folds).

The three species that are most geographically close to *C. altafissura* sp. nov. are *C. capillata* and *C. lamarckii* in NW Europe and *C. annasethe* off the Cape of Good Hope. The former species are located ~ 6,500 km from northern populations of *C. altafissura* sp. nov. off Côte d'Ivoire, while the latter is ~3,000 km from southern populations of *C. altafissura* sp. nov. off central Angola. In the case of *C. capillata* and *C. lamarckii* the species are separated by the Bay of Biscay, the upwelling centres off the Atlantic coast of the Iberian Peninsula and the Canary Current ecosystem, while *C. annasethe* is separated from *C. altafissura* sp. nov. by the Benguela upwelling ecosystem. Coastal waters in the Gulf of Guinea typically range from 24–30°C (Odekunle & Eludoyen 2008), whilst those experienced in the coastal upwelling ecosystems of the Canary and Benguela may routinely drop below 15°C (Gibbons *et al.* 2021). Both *C. capillata* and *C. lamarckii*, and *C. annasethe* (Figure 1), have rhopalial lappet clefts

that are markedly shorter than velar clefts, whilst the opposite is true for *C. altafissura* **sp. nov.** The coronal muscles of *C. capillata*, if not those of *C. lamarckii*, are obviously penetrated by gastrovascular pits, and the canal network in the marginal lappets of both species rarely display anastomosis, unlike those of *C. altafissura* **sp. nov.** Further, the coronal muscle fields in the latter species are widely separated by thickened septa, as *C. barkeri* Gershwin, Zeidler & Davie, 2010 (Gershwin *et al.* 2010), unlike those of the former two species. Comprehensive information for *C. annasethe* is lacking, but the number of tentacles per octant is much smaller even than the minimum number of tentacles observed here for *C. altafissura* **sp. nov.** (~80 per field for a specimen measuring 140 mm bell diameter).

Stiasny and van der Maaden (1943) proposed that species within the genus *Cyanea* can be broadly separated into a *capillata*-group and a *nozakii*-group, depending on whether the 16 radial septa are interrupted or not from origin to lappet margin (Figure 14). Species in the former group have complete septa that terminate, albeit sometimes indistinctly, in the lappets (Figure 14a), whilst those of the latter are repeatedly interrupted and effectively “fizzle out” before the base of lappets (Figure 14b). The radial septa of *C. altafissura* **sp. nov.** are of the *nozakii*-type and are similar to those described by Gershwin *et al.* (2010) for *C. barkeri*, originating as raised thickenings between coronal muscles (Figure 8). This latter feature appears indicative of species in the *nozakii*-group, if the illustrations summarised by Stiasny and van der Maaden (1943) are accurate. *Cyanea capillata* (Figure 14a), *C. lamarckii* and *C. annasethe* (Figure 1b), by contrast, belong to the *capillata*-group. The observation that *C. altafissura* **sp. nov.** is a member of the *nozakii*-group is supported, in part, by the molecular data (Figures 11 and 12, Appendix 3) with the species either sitting as a sister group to *C. nozakii* (Figure 11) or outside of the *capillata*-group, along with *C. nozakii* (Figure 12). Both analyses exhibit strong bootstrap support and the resolution of the monophyly of the *nozakii*-group would likely be strengthened with the addition of more molecular samples to enhance the resolution and better explain the high levels of ITS variation.

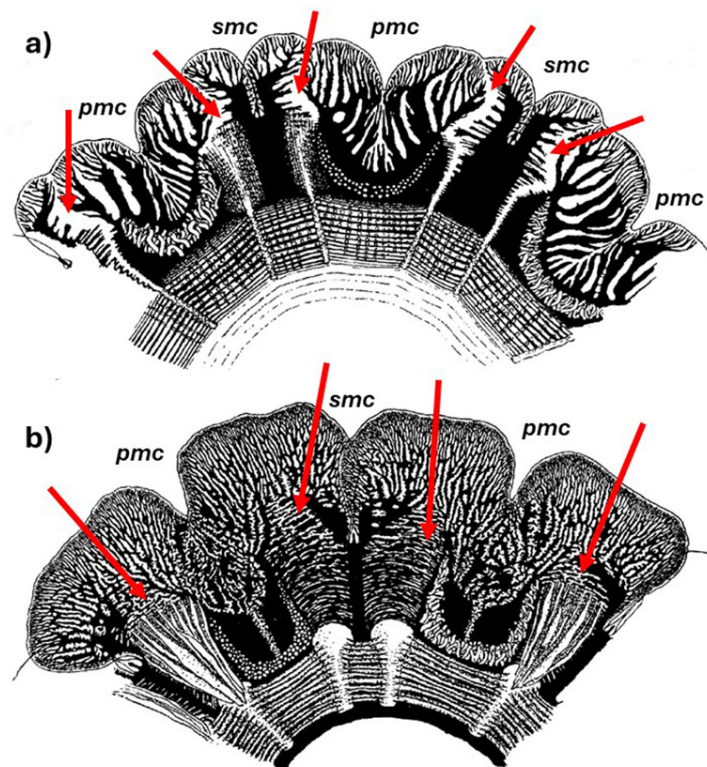


FIGURE 14. Plan diagrams of the subumbrella margin of the two subgroups of *Cyanea*. a) *Cyanea capillata*, *capillata*-group; b) *Cyanea nozakii*, *nozakii*-group. Red arrows indicate the radial septa, which are complete in the former and interrupted in the latter. *pmc* = primary marginal cleft, *smc* = secondary marginal cleft. From Stiasny and van der Maaden (1943).

Although several species of *Cyanea* are found in the cold temperate waters of the North Atlantic, tropical species tend to be concentrated in the Indo-West Pacific. None have been formally described from either the Eastern Pacific or the tropical Atlantic. We say formally described, because Kramp (1959) recorded three specimens of *C. capillata* that were collected off Sierra Leone and one off the mouth of the Congo River, DRC, during the

Belgian oceanographical expeditions to the Atlantic coasts of Africa during the years 1948–1949 and 1955. No descriptions of the material are provided by Kramp (1959), though he does note that “there is some uncertainty as to the limitation of the various «species» of *Cyanea* which have been described, but presumably *C. capillata* with its local varieties has an almost world-wide distribution in coastal waters” (Kramp 1959: 25). We now know the latter statement to be false, as noted earlier, and it is therefore very likely that Kramp’s (1959) specimens from the west coast of Africa were of the species described here for the first time. We stress, however, that the same cannot be said of the specimen he recorded in the same species account from the coast of Nova Scotia!

That *C. alatafissura* **sp. nov.** belongs to the *nozakii*-group, and not the *capillata*-group, poses interesting questions about its origin, which must either have been via the Tethys/Mediterranean Sea or around the coast of the Africa. No species of *Cyanea* are currently found in the Mediterranean Sea, though *C. nozakii* has been recorded off the SW coast of India and in the Bay of Bengal (Siddique *et al.* 2023), and while Cornelius (1997) reports the presence of *C. nozakii* off the coast of East Africa, the basis of his observation is unclear. If *C. nozakii* is indeed present in the Western Indian Ocean, then dispersal of a common ancestor around the southern African continent into the Atlantic is not unreasonable, as has been suggested for *Pelagia*, *Chrysaora* and *Rhizostoma* (Gibbons *et al.* 2021). Food for thought.

Acknowledgements

We would like to thank regional colleagues as well as the officers and crew of the RV *Dr. Fridtjof Nansen* for their assistance in the collection of specimens. Special words of thanks are owed to Gabriella Bianchi for encouraging the inclusion of jellyfish in the EAF Nansen Programme. We are grateful to the two anonymous reviewers for the obvious time and effort they put into reviewing an earlier draft of the manuscript, and their comments have greatly improved it: thanks. We are indebted to Peter van Heusden at the South African National Bioinformatics Institute, UWC, for running our COI data through his super computers. We would like to acknowledge the financial and logistic support provided by the National Research Foundation (NRF), the University of the Western Cape, the EAF Nansen Programme and PRIMALearn.

Contributions

Concept and funding MJG; data collection and analysis YS, MKB, MJG; writing YS, MKB, MJG; reviewing YS, MKB, MJG; editing MJG.

References

- Agassiz, L. (1862) *Contributions to the Natural History of the United States of America. Vol. IV. Pt. III. Discophorae. Pt. IV. Hydroidae. Pt. V. Homologies of the Radiata.* Little Brown Trubner, Boston, London, 380 pp.
- Anderson, M.J., Gorley, R.N. & Clarke, K.R. (2008) *PERMANOVA+ for PRIMER: Guide to Software and Statistical Methods.* PRIMER-E, Plymouth, 214 pp.
- Bayer, F.M., Eschscholtz, J.F., Guimpel, F., & Heyn. (1829) *System der Acalephen: eine ausführliche Beschreibung aller meduse. nartigen Strahlthiere.* bei Ferdinand Dümmler, Berlin, VI + 190 pp., 26 tabs.
<https://doi.org/10.5962/bhl.title.64070>
- Brandt, J.F. (1835) *Prodromus descriptionis animalium ab H. Mertensio observatorum: fascic. I. Polypos, Acalephas Discophoras et Siphonophoras, nec non Echinodermata continens / auctore, Johanne Friderico Brandt.* l'Academie imperiale des sciences de St. Petersbourg, St. Petersbourg, 72 pp. [pp. 204–275]
<https://doi.org/10.5962/bhl.title.10196>
- Brown, M.K. & Gibbons, M.J. (2022) Cautioning the move from morphology to molecules in the taxonomy of Metazoa: Comments on Lawley *et al.* (PeerJ 2021; 9, e11954) and a plea for considered integration. *South African Journal of Science*, 118, 1–2.
<https://doi.org/10.17159/sajs.2022/12590>
- Brown, M., Scorrano, S., Kuplik, Z., Kuyper, D., Ras, V., Thibault, D., Engelbrecht, A. & Gibbons, M.J. (2021) A new macromedusa from the coast of Mozambique: *Aurelia mozambica* sp. nov. (Scyphozoa: Ulmaridae). *Zootaxa*, 4933 (2), 263–276.

<https://doi.org/10.11646/zootaxa.4933.2.5>

- Collins, A.G. & Morandini, A.C. (2024) World List of Scyphozoa. *Cyanea* Péron & Lesueur, 1810. Accessed through: World Register of Marine Species. Available from: <https://www.marinespecies.org/aphia.php?p=taxdetails&id=135259> (accessed 27 February 2024)
- Dawson, M.N. & Jacobs, D. K. (2001) Molecular Evidence for Cryptic Species of *Aurelia aurita* (Cnidaria, Scyphozoa). *The Biological Bulletin*, 200 (1), 92–96.
<https://doi.org/10.2307/1543089>
- Dawson, M.N. (2005a) *Cyanea capillata* is not a cosmopolitan jellyfish: morphological and molecular evidence for *Cyanea annaskala* and *Cyanea rosea* (Scyphozoa: Semaestomeae: Cyaneidae) in Southeastern Australia. *Invertebrate Systematics*, 19, 361–370.
<https://doi.org/10.1071/IS03035>
- Dawson, M.N. (2005b) Renaissance taxonomy: integrative evolutionary analyses in the classification of Scyphozoa. *Journal of the Marine Biological Association of the United Kingdom*, 85 (3), 733–739.
<https://doi.org/10.1017/s0025315405011641>
- de Lafontaine, Y. & Leggett, W. (1989) Changes in size and weight of hydromedusae during formalin preservation. *Bulletin of Marine Science*, 44, 1129–1137.
- Dong, J., Sun, M., Wang, B. & Liu, H. (2008) Comparison of life cycles and morphology of *Cyanea nozakii* and other scyphozoans. *Plankton and Benthos Research*, 3, 118–124.
<https://doi.org/10.3800/pbr.3.118>
- Eytan, R.I., Hayes, M.L., Arbour-Reily, P., Miller, M.W. & Hellberg, M.E. (2009) Nuclear sequences reveal mid-range isolation of an imperilled deep-water coral population. *Molecular Ecology*, 18 (11), 2375–2389.
<https://doi.org/10.1111/j.1365-294x.2009.04202.x>
- Eschscholtz, F. (1829) n.k. In: System der Acalephen. Eine ausführliche Beschreibung aller medusenartigen Strahltiere. Ferdinand Dümmler, Berlin, pp. 70–71. [<https://www.biodiversitylibrary.org/page/10665047>]
<https://doi.org/10.5962/bhl.title.64070>
- F.A.O. (2020) *The EAF-Nansen Programme Science Plan. Supporting the Application of the Ecosystem Approach to Fisheries (EAF) management considering climate and pollution impacts (2017–2021)*. F.A.O., Rome, 2 pp.
- Felsenstein, J. (1985) Confidence limits on phylogenies: An approach using the bootstrap. *Evolution*, 39, 783–791.
<https://doi.org/10.1111/j.1558-5646.1985.tb00420.x>
- Folmer, O., Black, M., Hoeh, W., Lutz, R. & Vrijenhoek, R. (1994) DNA primers for amplification of mitochondrial cytochrome *c* oxidase subunit I from diverse metazoan invertebrates. *Molecular Marine Biology and Biotechnology*, 3, 294–299.
- Gershwin, L., Zeidler, W. & Davie, P. (2010) Medusae (Cnidaria) of Moreton Bayo, Queensland, Australia. Medusae (Cnidaria) of Moreton Bay, Queensland, Australia. *Memoirs of the Queensland Museum*, 54 (3), 47–108.
- Gibbons, M.J. (2024) Jellyfish, People and the United Nation’s Sustainable Development Goals. *Journal of the Marine Biological Association of India*. [submitted]
- Gibbons, M.J., Morandini, A.C., Straehler-Pohl, I. & Bezio, N. (2022) *Identification guide to macro jellyfishes of West Africa*. Food and Agriculture Organisation of the United Nations, Rome, 193 pp.
- Haacke, W. (1887) Die Scyphomedusen des St. Vincent Golfes. *Jenaische Zeitschrift für Naturwissenschaft*, 20, 605–614, 3 pls.
- Haeckel, E. (1880) 2: System der Acraspeden. In: *Das System der Medusen. I*. Gustav Fischer, Jena, pp. 361–672.
- Hellberg, M.E. (2006) No variation and low synonymous substitution rates in coral mtDNA despite high nuclear variation. *BMC Evolutionary Biology*, 6 (1), 24.
<https://doi.org/10.1186/1471-2148-6-24>
- Holst, S. & Laakmann, S. (2014) Morphological and molecular discrimination of two closely related jellyfish species, *Cyanea capillata* and *C. lamarckii* (Cnidaria, Scyphozoa), from the northeast Atlantic. *Journal of Plankton Research*, 36 (1), 48–63
<https://doi.org/10.1093/plankt/fbt093>
- Jarms, G. & Morandini, A.C. (2019) *World Atlas of Jellyfish: Scyphozoa except Stauromedusae*. Dölling Und Galitz, München, 816 pp.
- Kishinouye, K. (1902) Some new scyphomedusae of Japan. In: *Journal of the College of Science. Vol. 17*. Tokyo Imperial University, Tokyo, pp. 1–17.
- Kishinouye, K. (1910) Some medusae of Japanese waters. In: *The Journal of the College of Science. Vol. 27*. Imperial University of Tokyo, pp. 1–35.
<https://repository.dl.itc.u-tokyo.ac.jp/records/37810>
- Koichiro, T., Stecher, G. & Kumar, S. (2021) MEGA11: Molecular Evolutionary Genetics Analysis version 11. *Molecular Biology and Evolution*, 38, 3022–3027.
<https://doi.org/10.1093/molbev/msab120>
- Kolbasova, G.D., Zalevsky, A.O., Gafurov, A., Gusev, F., Ezhova, M.A., Zheludkevich, A.A., Konovalova, O.P., Kosobokova, K., Kotlov, N., Lanina, N.O., Lapashina, A.S., Medvedev, D.O., Nosikova, K.S., Nuzhdina, E.O., Bazykin, G.A. & Neretina, T.V. (2015) A new species of *Cyanea* jellyfish sympatric to *Cyanea capillata* in the White Sea. *Polar Biology*, 38 (9), 1439–1451.

- <https://doi.org/10.1007/s00300-015-1707-y>
- Kramp, P.L. (1961) Synopsis of the medusae of the world. *Journal of Marine Biological Association of the United Kingdom*, 40, 1–469.
<https://doi.org/10.1017/s0025315400007347>
- Lawley, J.W., Gamero-Mora, E., Maronna, M.M., Chiaverano, L.M., Stampar, S.N., Hopcroft, R.R., Collins, A.G. & Morandini, A.C. (2021) The importance of molecular characters when morphological variability hinders diagnosability: Systematics of the moon jellyfish genus *Aurelia* (Cnidaria: Scyphozoa). *PeerJ*, 9, e11954.
<https://doi.org/10.7717/peerj.11954>
- Linnaeus, C. (1758) *Systema naturae per regna tria naturae, secundum classes, ordines, genera, species cum charact-eribus, differentiis, synonymis, locis. Editio decima, reformata. 10th Edition*. Laurentii Salvii, Holmiae, 824 pp.
<https://doi.org/10.5962/bhl.title.542>
- Maran, B.A.V., Aungtonya, C., Hoe, C.C., Metillo, E.B., Miyake, H., Iesa, I., Arsiranant, I., Karunarathne, K.D., Densing, L.A.F., De Croos, M.D.S.T. & Rizman-Idid, M. (2021) *Field Guide to the Jellyfish of Western Pacific*. Centre for Marine and Coastal Studies, Universiti Sains Malaysia, Penang, 145 pp.
- Mayer, A.G. (1910) Volume III: Schyphomedusae. In: Mayer, A.G., *Medusae of the world*. Carnegie Institute, Washington, pp. 499–735.
<https://doi.org/10.5962/bhl.title.5996>
- Odekunle, T.O. & Eludoyin, A.O. (2008) Sea surface temperature patterns in the Gulf of Guinea: their implications for the spatio-temporal variability of precipitation in West Africa. *International Journal of Climatology*, 28 (11), 1507–1517.
<https://doi.org/10.1002/joc.1656>
- Péron, F. & Lesueur, C.A. (1810) Tableau des caractères génériques et spécifiques de toutes les espèces de Méduses connues jusqu'à ce jour. *Annales du Muséum National d'Histoire Naturelle, Paris*, 14, 325–366.
- Pourjomah, F., Shokri, M.R., Rajabi-Maham, H., Rezai, H. & Maghsoudlou, E. (2017) New records of the scyphozoan medusae (Cnidaria: Scyphozoa) in the north of Gulf of Oman, Iran. *Marine Biodiversity*, 48 (4), 2193–2202.
<https://doi.org/10.1007/s12526-017-0683-6>
- Quoy, J., Cyanea, R. & Gaimard, J.P. (1824) *Voyage autour de monde, entrepris par ordre du roi. Exécuté sur l'Uranie et la Physicienne, pendant 1817–20. Zoologie 4*. Chez Pillet Aîné, Imprimeur-Libraire, Paris, 712 pp.
- Ramhaut, A. (2009) FigTree. Version 1.4.1. Available from: <http://tree.bio.ed.ac.uk/software/figtree/> (accessed 26 February 2024)
- Ras, V., Neethling, S., Engelbrecht, A., Morandini, A., Bayha, K., Skrypzeck, H. & Gibbons, M. (2020) There are three species of *Chrysaora* (Scyphozoa: Discomedusae) in the Benguela upwelling ecosystem, not two. *Zootaxa*, 4778 (3), 401–438.
<https://doi.org/10.11646/zootaxa.4778.3.1>
- Richards, R. (2008) The tragic sense of life: Ernst Haeckel and the struggle over evolutionary thought. *Choice Reviews Online*, 46 (03), 46–1447.
<https://doi.org/10.7208/chicago/9780226712192.001.0001>
- Ronquist, F. & Huelsenbeck, J.P. (2003) MrBayes 3: Bayesian phylogenetic inference under mixed models. *Bioinformatics*, 19, 1572–1574.
<https://doi.org/10.1093/bioinformatics/btg180>
- Russell, F.S. (1970) *The Medusae of the British Isles. II Pelagic Scyphozoa with a Supplement to the First Volume on Hydromedusae*. Cambridge University Press, Cambridge, 284 pp.
- Siddique, A., Basu, S., Prasad, H., Bhowal, A., Changarangath, P.R. & Purushothaman, J. (2023) Morphological and molecular characterisation of ghost jellyfish *Cyanea nozakii* (Cnidaria: Scyphozoa) forming a swarm in the Bay of Bengal, Indian Ocean. *Regional Studies in Marine Science*, 68, 103271.
<https://doi.org/10.1016/j.rsma.2023.103271>
- Stiasny, G. (1919) Die Scyphomedusen-Sammlung des Naturhistorischen Reichsmuseums in Leiden. II. Stauromedusae, Coronatae, Semaestomeae. *Zoologische Mededeelingen*, 4, 66–99.
- Stiasny, G. (1921) Studien über rhizostomeen. *Capita Zoologica*, 1 (2), 1–179, 5 pls.
- Stiasny, G. & van der Maaden, H. (1943) Über Scyphomedusen aus dem Ochotskischen und Kamtschatka Meer nebst einer Kritik der Genera *Cyanea* and *Desmonema*. *Zoologische Jahrbucher*, 76, 227–266.
- von Lendenfeld, R. (1882) Über Coelenteraten der Südsee. I. *Cyanea annaskala*, sp. n. *Zeitschrift für Wissenschaftliche Zoologie*, 37, 465–552.

APPENDIX 1a. Table showing locality information for specimens of *C. capillata*, *C. tzetlinii*, *C. annaskala*, *C. lamarckii*, *C. nozakii*, and *C. rosea* used in the genetic analyses of this study. GenBank accession numbers are provided for COI gene regions.

Species	Location	Area	Accession number
<i>C. altafissura</i> sp. nov.	4°N, 2°W	Akwidaa, Ahanta West Municipal District, Ghana	PQ185525
<i>C. capillata</i>	66.34 N 33.08 E	North Atlantic, Russia	KM281996
<i>C. capillata</i>	66.34 N 33.08 E	North Atlantic, Russia	KM281974
<i>C. capillata</i>	66.34 N 33.08 E	North Atlantic, Russia	KM281982
<i>C. capillata</i>	66.34 N 33.08 E	North Atlantic, Russia	KM281980
<i>C. capillata</i>	58.792N 93.751W	Canada: Manitoba, Churchill	MG421412
<i>C. capillata</i>	66.34 N 33.08E	North Atlantic, Russia	KM281972
<i>C. capillata</i>	66.55379 N 33.10473 E	North Atlantic, Russia	KM983293
<i>C. capillata</i>	66.55379 N 33.10473 E	North Atlantic, Russia	KM983291
<i>C. capillata</i>	66.55379 N 33.10473 E	North Atlantic, Russia	KM983284
<i>C. capillata</i>	66.55379 N 33.10473 E	North Atlantic, Russia	KM983282
<i>C. capillata</i>	67.6333 N 12.1667 W	Atlantic Ocean: North Atlantic	JX995340
<i>C. capillata</i>	54.4352 N 10.1701 E	Baltic Sea	JX995342
<i>C. capillata</i>	54.4352 N 10.1701 E	Baltic Sea	JX995343
<i>C. capillata</i>	54.4352 N 10.1701 E	Baltic Sea	JX995346
<i>C. capillata</i>	58.35 N 11.222 E	Sweden: Skagerrak	MG935310
<i>C. capillata</i>	58.875 N 93.8004 W	Canada: Manitoba, Churchill,	MG423233
<i>C. capillata</i>	58.792 N 93.751 W	Canada: Manitoba, Churchill	MG423436
<i>C. capillata</i>	-	Atlantic Ocean:Northeast Atlantic	HF930525
<i>C. capillata</i>	54.1863 N 7.9000 E	North Sea	JX995338
<i>C. capillata</i>	-	Norway: Raunefjorden	AY902911
<i>C. capillata</i> *	44.956 N 66.9278 W	Canada: New Brunswick, St. Andrews, Casco Bay Island	MG421890
<i>C. capillata</i> *	38.8763 N 76.5465 W	USA: Maryland, Anne Arundel County, Rhode River, Chesapeake Bay	MH087647
<i>C. tzetlinii</i>	66.34 N 33.08 E	North Atlantic, Russia	KM281987
<i>C. tzetlinii</i>	66.34 N 33.08 E	North Atlantic, Russia	KM281990
<i>C. tzetlinii</i>	66.34 N 33.08 E	North Atlantic, Russia	KM281994
<i>C. tzetlinii</i>	66.34 N 33.08 E	North Atlantic, Russia	KM281997
<i>C. tzetlinii</i>	66.34 N 33.08 E	North Atlantic, Russia	KM281993
<i>C. rosea</i>	-	South Pacific, Australia	AY902922
<i>C. rosea</i>	-	South Pacific, Australia	AY902921
<i>C. rosea</i>	-	South Pacific, Australia	AY902919
<i>C. rosea</i>	-	South Pacific, Australia	AY902920
<i>C. annaskala</i>	-	South Pacific, Tasmania	AY902914
<i>C. annaskala</i>	-	South Pacific, Tasmania	AY902915
<i>C. annaskala</i>	-	South Pacific, Tasmania	AY902916
<i>C. annaskala</i>	-	South Pacific, Tasmania	AY902923
<i>C. annaskala</i>	-	South Pacific, Tasmania	AY902917
<i>C. nozakii</i>	-	Indian Ocean	MH479115
<i>C. nozakii</i>	-	Indian Ocean	MH479116

.....Continued on the next page

APPENDIX 1a. (Continued)

Species	Location	Area	Accession number
<i>C. nozakii</i>	-	Indian Ocean	MH479112
<i>C. nozakii</i>	-	Indian Ocean	MH479113
<i>C. nozakii</i>	19.39 N 85.094 E	Indian Ocean, Bay of Bengal	ON184036
<i>C. nozakii</i>	19.25 N 84.93 E	Indian Ocean, Bay of Bengal	ON210095
<i>C. nozakii</i>	-	Iran: Chabahar Gulf	KY655794
<i>C. nozakii</i>	-	Iran: Chabahar Gulf	KY655796
<i>C. nozakii</i>	-	China	MZ007765
<i>C. nozakii</i>	-	China	MZ007762
<i>C. nozakii</i>	-	China	MZ007763
<i>C. nozakii</i>	-	China	MZ007760
<i>C. lamarekii</i>	57.65 N 11.75 E	North Atlantic, Sweden	MG935374
<i>C. lamarekii</i>	54.19 N 7.90 E	North Atlantic, North Sea	JX995362
<i>C. lamarekii</i>	58.35 N 11.22 E	North Atlantic, Sweden	MG935135
<i>C. lamarekii</i>	54.19 N 7.90 E	North Atlantic, North Sea	JX995357
<i>C. lamarekii</i>	54.57 N 7.15 E	North Atlantic, North Sea	JX995356
<i>C. lamarekii</i>	-	Atlantic Ocean: Northeast Atlantic	HF930523
<i>C. lamarekii</i>	58.35 N 11.222 E	Sweden: Skagerrak	MG935114
<i>C. lamarekii</i>	54.1863 N 7.9000 E	North Sea	JX995361
<i>C. lamarekii</i>	53.9491 N 6.7604 E	North Sea	JX995355
<i>C. lamarekii</i>	53.7645 N 8.0629 E	North Sea	JX995352
<i>C. lamarekii</i>	54.1863 N 7.9000 E	North Sea	JX995349
<i>C. lamarekii</i>	54.1863 N 7.9000 E	North Sea	JX995347
<i>Cyanea</i> sp.	66.55379 N 33.10473 E	Russia	KM983286
<i>Cyanea</i> sp.	59.493 N 151.646 W	USA: Alaska, Cook Inlet, Katchemak Bay	MF121108
<i>Cyanea</i> sp.	-	Canada: Nunavut, Igloolik	MG421562
<i>Cyanea</i> sp.	59.493 N 151.646 W	USA: Alaska, Cook Inlet, Katchemak Bay	MF121412
<i>Cyanea</i> sp.	66.55379 N 33.10473 E	Russia	KM983289
<i>Cyaneasp.</i>	54.1069 N 132.366 W	Canada: British Columbia, Haida Gwaii, Half Way Point, North end of QC	MG423131
<i>Cyanea</i> sp.	58.768 N 93.869 W	Canada: Manitoba, Churchill	MG423484
<i>D. dalmatinum</i>	-	North Atlantic, Turkey	HQ234616
<i>D. dalmatinum</i>	-	North Atlantic, Turkey	HQ234621
<i>D. dalmatinum</i>	-	North Atlantic, Turkey	HQ234617
<i>D. dalmatinum</i>	-	North Atlantic, Turkey	HQ234615

*Appears to be misidentified

APPENDIX 1b. Table showing locality information for specimens of *C. capillata*, *C. tzetlinii*, *C. annaskala*, *C. lamarckii*, *C. nozakii*, and *C. rosea* used in the genetic analyses of this study. GenBank accession numbers are provided for ITS gene regions

Species	Location	Area	Accession number
<i>C. altafissura</i> sp. nov	4°N, 2°W	Akwidaa, Ahanta West Municipal District, Ghana	PQ204435
<i>C. capillata</i>	66.34 N 33.08 E	North Atlantic, Russia	KM281971
<i>C. capillata</i>	66.34 N 33.08 E	North Atlantic, Russia	KM281970
<i>C. capillata</i>	66.34 N 33.08 E	North Atlantic, Russia	KM281969
<i>C. capillata</i>	66.34 N 33.08 E	North Atlantic, Russia	KM281965
<i>C. capillata</i>	66.34 N 33.08 E	North Atlantic, Russia	KM281963
<i>C. tzetlinii</i>	66.34 N 33.08 E	North Atlantic, Russia	KM281967
<i>C. tzetlinii</i>	66.34 N 33.08 E	North Atlantic, Russia	KM281966
<i>C. tzetlinii</i>	66.34 N 33.08 E	North Atlantic, Russia	KM281964
<i>C. tzetlinii</i>	66.34 N 33.08 E	North Atlantic, Russia	KM281968
<i>C. tzetlinii</i>	66.34 N 33.08 E	North Atlantic, Russia	KM281960
<i>C. rosea</i>	-	South Pacific, Australia	AY903059
<i>C. rosea</i>	-	South Pacific, Australia	AY903057
<i>C. rosea</i>	-	South Pacific, Australia	AY903058
<i>C. rosea</i>	-	South Pacific, Australia	AY903060
<i>C. annaskala</i>	-	South Pacific, Tasmania	AY903062
<i>C. annaskala</i>	-	South Pacific, Tasmania	AY903064
<i>C. annaskala</i>	-	South Pacific, Tasmania	AY903061
<i>C. annaskala</i>	-	South Pacific, Tasmania	AY903063
<i>C. annaskala</i>	-	South Pacific, Tasmania	AY903065
<i>C. nozakii</i>	-	Pacific Ocean	AB377554
<i>C. nozakii</i>	-	Pacific Ocean	AB377552
<i>C. nozakii</i>	-	Pacific Ocean	AB377551
<i>C. nozakii</i>	-	Pacific Ocean	AB377553
<i>D. dalmatinum</i>	-	North Atlantic, Turkey	HQ234643
<i>D. dalmatinum</i>	-	North Atlantic, Turkey	HQ234642
<i>D. dalmatinum</i>	-	North Atlantic, Turkey	HQ234641
<i>D. dalmatinum</i>	-	North Atlantic, Turkey	HQ234647

APPENDIX 2. Mean Pairwise genetic distances for the mtDNA (COI) (lower triangle) and nuDNA (ITS1) (upper triangle) for *Cyanea* species.

	<i>C. capillata</i>	<i>C. annaskala</i>	<i>C. rosea</i>	<i>C. altafissura</i> sp. nov.	<i>C. lamarckii</i>	<i>C. tzetlini</i>	<i>C. nozakii</i>	<i>C. capillata</i> (Questionable)	<i>Cyanea</i> sp.
<i>C. capillata</i>	--	0,027	0,040	0,162		0,039	0,159		
<i>C. annaskala</i>	0,056	--	0,042	0,224		0,024	0,171		
<i>C. rosea</i>	0,051	0,046	--	0,222		0,050	0,175		
<i>C. altafissura</i> sp. nov.	0,130	0,124	0,119	--		0,149	0,144		
<i>C. lamarckii</i>	0,067	0,068	0,064	0,122	--				
<i>C. tzetlini</i>	0,022	0,052	0,054	0,127	0,070	--	0,144		
<i>C. nozakii</i>	0,123	0,124	0,119	0,126	0,126	0,113	--		
<i>C. capillata</i> (Questionable)	0,071	0,072	0,065	0,118	0,008	0,072	0,119	--	
<i>Cyanea</i> sp.	0,006	0,054	0,054	0,129	0,069	0,019	0,124	0,070	--

APPENDIX 3. A midpoint rooted maximum likelihood tree of *Cyanea* spp. COI sequences, with a number of additional *C. nozakii* sequences added. Bootstrap support values (ML) are given above branches, with posterior probabilities (BY) given below branches.

